Theoretical approach to thermal noise caused by an inhomogeneously distributed loss: Physical insight by the advanced modal expansion

Kazuhiro Yamamoto,* Masaki Ando, Keita Kawabe, and Kimio Tsubono

Department of Physics, the University of Tokyo, 7-3-1 Hongo, Bunkyo-ku, Tokyo 113-0033, Japan

(Received 6 December 2006; published 17 April 2007)

We modified the modal expansion, which is the traditional method used to calculate thermal noise. This advanced modal expansion provides physical insight about the discrepancy between the actual thermal noise caused by inhomogeneously distributed loss and the traditional modal expansion. This discrepancy comes from correlations between the thermal fluctuations of the resonant modes. The thermal-noise spectra estimated by the advanced modal expansion are consistent with the results of measurements of thermal fluctuations caused by inhomogeneous losses.

DOI: 10.1103/PhysRevD.75.082002 PACS numbers: 04.80.Nn, 05.40.Jc, 06.30.Ft, 62.40.+i

I. INTRODUCTION

Thermal fluctuation is one of the fundamental noise sources in precise measurements. For example, the sensitivity of interferometric gravitational-wave detectors [1–4] is limited by the thermal noise of the mechanical components. The calculated thermal fluctuations of rigid cavities have coincided with the highest laser frequency stabilization results ever obtained [5,6]. It is important to evaluate the thermal motion when studying the noise property. The (traditional) modal expansion [7] has been commonly used to calculate the thermal noise of elastic systems. However, recent experiments [8–13] have revealed that modal expansion is not correct when the mechanical dissipation is distributed inhomogeneously. In some theoretical studies [14–17], calculation methods that are completely different from modal expansion have been developed. These methods are supported by the experimental results of inhomogeneous loss [9,11–13]. However, even when these method were used, the physics of the discrepancy between the actual thermal noise and the traditional modal expansion was not fully understood.

In this paper, another method to calculate the thermal noise is introduced [17]. This method, advanced modal expansion, is a modification of the traditional modal expansion (this improvement is a general extension of a discussion in Ref. [18]). The thermal-noise spectra estimated by this method are consistent with the results of experiments concerning inhomogeneous loss [8,12]. It provides information about the disagreement between the thermal noise and the traditional modal expansion. We present the details of these topics in the following sections.

*Electronic address: yamak@icrr.u-tokyo.ac.jp
Present address: Gravitational wave group, Institute for Cosmic Ray Research, the University of Tokyo, 5-1-5 Kashiwa-no-Ha, Kashiwa, Chiba 277-8582, Japan.

II. OUTLINE OF ADVANCED MODAL EXPANSION

A. Review of the traditional modal expansion

The thermal fluctuation of the observed coordinate, X, of a linear mechanical system is derived from the fluctuation-dissipation theorem [19–21],

$$G_X(f) = -\frac{4k_B T}{\omega}\,\mathrm{Im}[H_X(\omega)], \tag{1}$$

$$H_X(\omega) = \frac{\tilde{X}(\omega)}{\tilde{F}(\omega)}, \tag{2}$$

$$\tilde{X}(\omega) = \frac{1}{2\pi}\int_{-\infty}^{\infty} X(t)\exp(-i\omega t)dt, \tag{3}$$

where f ($= \omega/2\pi$), t, k_B, and T, are the frequency, time, Boltzmann constant and temperature, respectively. The functions (G_X, H_X, and F) are the (single-sided) power spectrum density of the thermal fluctuation of X, the transfer function, and the generalized force, which corresponds to X. In the traditional modal expansion [7], in order to evaluate this transfer function, the equation of motion of the mechanical system without any loss is decomposed into those of the resonant modes. The details are as follows.

The definition of the observed coordinate, X, is described as

$$X(t) = \int \boldsymbol{u}(\boldsymbol{r}, t)\cdot\boldsymbol{P}(\boldsymbol{r})dS, \tag{4}$$

where $\boldsymbol{u}$ is the displacement of the system and $\boldsymbol{P}$ is a weighting function that describes where the displacement is measured. For example, when mirror motion is observed using a Michelson interferometer, as in Fig. 1, X and $\boldsymbol{u}$ represent the interferometer output and the displacement of the mirror surface, respectively. The vector $\boldsymbol{P}$ is parallel to the beam axis. Its norm is the beam-intensity profile [14]. The equation of motion of the mechanical system without dissipation is expressed as

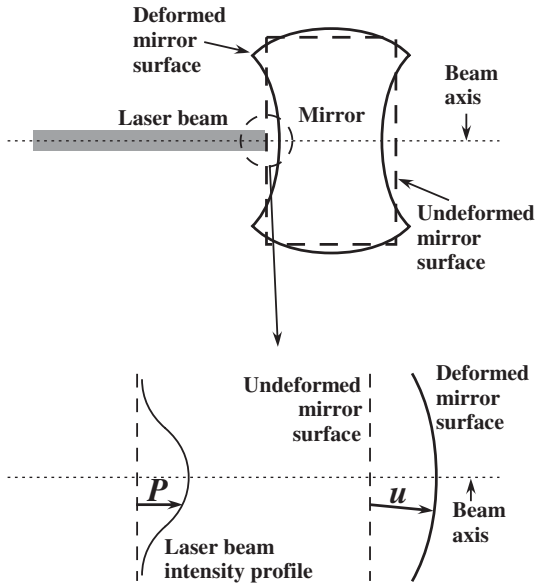

FIG. 1. Example of the definition of the observed coordinate, X, in Eq. (4). The mirror motion is observed using a Michelson interferometer. The coordinate X is the output of the interferometer. The vector $\boldsymbol{u}$ represents the displacement of the mirror surface. The field $\boldsymbol{P}$ is parallel to the beam axis. Its norm is the beam-intensity profile [14].

$$\rho \frac{\partial^2 \boldsymbol{u}}{\partial t^2} - \mathcal{L}[\boldsymbol{u}] = F(t)\boldsymbol{P}(\boldsymbol{r}), \tag{5}$$

where ρ is the density and $\mathcal{L}$ is a linear operator. The first and second terms on the left-hand side of Eq. (5) represent the inertia and the restoring force of the small elements in the mechanical oscillator, respectively. The solution of Eq. (5) is the superposition of the basis functions

$$\boldsymbol{u}(\boldsymbol{r}, t) = \sum_n \boldsymbol{w}_n(\boldsymbol{r}) q_n(t). \tag{6}$$

The functions $\boldsymbol{w}_n$ and q_n represent the displacement and time development of the n-th resonant mode, respectively. The basis functions $\boldsymbol{w}_n$ are solutions of the eigenvalue problem, written as

$$\mathcal{L}[\boldsymbol{w}_n(\boldsymbol{r})] = -\rho \omega_n{}^2 \boldsymbol{w}_n(\boldsymbol{r}), \tag{7}$$

where ω_n is the angular resonant frequency of the n-th mode. The displacement, $\boldsymbol{w}_n$, is the component of an orthogonal complete system, and is normalized to satisfy the condition

$$\int \boldsymbol{w}_n(\boldsymbol{r}) \cdot \boldsymbol{P}(\boldsymbol{r}) dS = 1. \tag{8}$$

The formula of the orthonormality is described as

$$\int \rho \boldsymbol{w}_n(\boldsymbol{r}) \cdot \boldsymbol{w}_k(\boldsymbol{r}) dV = m_n \delta_{nk}. \tag{9}$$

The parameter m_n is called the effective mass of the mode [8,22–24]. The tensor δ_{nk} is the Kronecker's δ symbol.

Putting Eq. (6) into Eq. (4), we obtain a relationship between X and q_n using Eq. (8):

$$X(t) = \sum_n q_n(t). \tag{10}$$

In short, coordinate X is a superposition of those of the modes q_n. In order to decompose the equation of motion, Equation (5), Eq. (6) is substituted for $\boldsymbol{u}$ in Eq. (5). Equation (5) is multiplied by $\boldsymbol{w}_n$ and then integrated over all of the volume using Eqs. (7)–(9). The result is that the equation of motion of the n-th mode, q_n, is the same as that of a harmonic oscillator on which force $F(t)$ is applied. After modal decomposition, the dissipation term is added to the equation of each mode. The equation of the n-th mode is written as

$$-m_n \omega^2 \tilde{q}_n + m_n \omega_n{}^2 [1 + \mathrm{i}\phi_n(\omega)] \tilde{q}_n = \tilde{F}, \tag{11}$$

in the frequency domain. The function ϕ_n is the loss angle, which represents the dissipation of the n-th mode [7]. The transfer function, H_X, derived from Eqs. (2), (10), and (11) is the summation of those of the modes H_n,

$$H_X(\omega) = \frac{\tilde{X}}{\tilde{F}} = \sum_n \frac{\tilde{q}_n}{\tilde{F}} \left(= \sum_n H_n \right) = \sum_n \frac{1}{-m_n \omega^2 + m_n \omega_n{}^2 [1 + \mathrm{i}\phi_n(\omega)]}. \tag{12}$$

According to Eqs. (1) and (12), the power spectrum density G_X is the summation of the power spectrum G_{q_n} of q_n

$$G_X(f) = \sum_n G_{q_n} = \sum_n \frac{4k_B T}{m_n \omega} \frac{\omega_n{}^2 \phi_n(\omega)}{(\omega^2 - \omega_n{}^2)^2 + \omega_n{}^4 \phi_n{}^2(\omega)}. \tag{13}$$

B. Equation of motion in an advanced modal expansion

In the traditional modal expansion, the dissipation term is introduced after decomposition of the equation of motion without any loss. On the contrary, in an advanced modal expansion, the equation with the loss is decomposed [17,25]. If the loss is sufficiently small, the expansion process is similar to that in the perturbation theory of quantum mechanics [26]. The equation of q_n is expressed as

$$-m_n \omega^2 \tilde{q}_n + m_n \omega_n{}^2 [1 + \mathrm{i}\phi_n(\omega)] \tilde{q}_n + \sum_{k \neq n} \mathrm{i}\alpha_{nk}(\omega) \tilde{q}_k = \tilde{F}, \tag{14}$$

$$\phi_n(\omega) = \frac{\alpha_{nn}}{m_n \omega_n{}^2}. \tag{15}$$

The third term in Eq. (14) is the difference between the advanced, Eq. (14), and traditional, Eq. (11), modal expansions. Since this term is a linear combination of the motions of the other modes, it represents the couplings

between the modes. The magnitude of the coupling α_{nk} depends on the property and the distribution of the loss (described below).

C. Details of coupling

Let us consider the formulae of the couplings caused by the typical inhomogeneous losses, the origins of which exist outside and inside the material (viscous damping and structure damping, respectively) [17]. Regarding most of the external losses, for example, the eddy-current damping and residual gas damping are of the viscous type [7]. The friction force of this damping is proportional to the velocity. Inhomogeneous viscous damping introduces a friction force $i\omega\rho\Gamma(\boldsymbol{r})\tilde{\boldsymbol{u}}(\boldsymbol{r})$ into the left-hand side of the equation of motion, Eq. (5), in the frequency domain. The function $\Gamma(\geq 0)$ represents the strength of the damping. The equation of motion with the dissipation term, $i\omega\rho\Gamma(\boldsymbol{r})\tilde{\boldsymbol{u}}(\boldsymbol{r})$, is decomposed. Since the loss is small, the basis functions of the equation without loss are available [26]. Equation (6) is put into the equation of motion along with the inhomogeneous viscous damping. This equation multiplied by $\boldsymbol{w}_n$ is integrated. The coupling of this dissipation is written in the form

$$\alpha_{nk} = \omega \int \rho\Gamma(\boldsymbol{r})\boldsymbol{w}_n(\boldsymbol{r}) \cdot \boldsymbol{w}_k(\boldsymbol{r})dV = \alpha_{kn}. \tag{16}$$

In most cases, the internal loss in the material is expressed using the phase lag, $\phi(\geq 0)$, between the strain and the stress [7]. The magnitude of the dissipation is proportional to this lag. The phase lag is almost constant against the frequency [7] in many kinds of materials (structure damping). In the frequency domain, the relationship between the strain and the stress (the generalized Hooke's law) in an isotropic elastic body is written as [7,14,17,27]

$$\begin{aligned}\tilde{\sigma}_{ij} &= \frac{E_0[1 + i\phi(\boldsymbol{r})]}{1 + \sigma}\left(\tilde{u}_{ij} + \frac{\sigma}{1 - 2\sigma}\sum_l \tilde{u}_{ll}\delta_{ij}\right) \\ &= [1 + i\phi(\boldsymbol{r})]\tilde{\sigma}'_{ij},\end{aligned} \tag{17}$$

$$u_{ij} = \frac{1}{2}\left(\frac{\partial u_i}{\partial x_j} + \frac{\partial u_j}{\partial x_i}\right), \tag{18}$$

where E_0 is Young's modulus and σ is the Poisson ratio; σ_{ij} and u_{ij} are the stress and strain tensors, respectively. The tensor $\tilde{\sigma}'_{ij}$ is the real part of the stress $\tilde{\sigma}_{ij}$. It represents the stress when the structure damping vanishes. The value, u_i, is the i-th component of $\boldsymbol{u}$. The equation of motion of an elastic body [27] in the frequency domain is expressed as

$$-\rho\omega^2\tilde{u}_i - \sum_j \frac{\partial\tilde{\sigma}_{ij}}{\partial x_j} = \tilde{F}P_i(\boldsymbol{r}), \tag{19}$$

where P_i is the i-th component of $\boldsymbol{P}$. From Eqs. (17) and (19), an inhomogeneous structure damping term is obtained, $-i\sum_j \partial\phi(\boldsymbol{r})\tilde{\sigma}'_{ij}/\partial x_j$. The equation of motion with the inhomogeneous structure damping is decomposed in the same manner as that of the inhomogeneous viscous damping. The coupling is calculated using integration by parts and Gauss' theorem [27]

$$\begin{aligned}\alpha_{nk} &= -\int \sum_{i,j} w_{n,i}\frac{\partial\phi(\boldsymbol{r})\sigma_{k,ij}}{\partial x_j}dV \\ &= -\int \sum_{i,j}\frac{\partial w_{n,i}\phi(\boldsymbol{r})\sigma_{k,ij}}{\partial x_j}dV + \int \sum_{i,j}\frac{\partial w_{n,i}}{\partial x_j}\phi(\boldsymbol{r})\sigma_{k,ij}dV \\ &= -\int \sum_{i,j} w_{n,i}\phi(\boldsymbol{r})\sigma_{k,ij}n_j dS + \int \sum_{i,j}\frac{\partial w_{n,i}}{\partial x_j}\phi(\boldsymbol{r})\sigma_{k,ij}dV \\ &= \int \frac{E_0\phi(\boldsymbol{r})}{1+\sigma}\left[\sum_{i,j}\frac{\partial w_{n,i}}{\partial x_j}\left(w_{k,ij} + \frac{\sigma}{1-2\sigma}\sum_l w_{k,ll}\delta_{ij}\right)\right]dV \\ &= \int \frac{E_0\phi(\boldsymbol{r})}{1+\sigma}\left(\sum_{i,j} w_{n,ij}w_{k,ij} + \frac{\sigma}{1-2\sigma}\sum_l w_{n,ll}\sum_l w_{k,ll}\right)dV \\ &= \alpha_{kn},\end{aligned} \tag{20}$$

where $w_{n,i}$ and n_i are the i-th components of $\boldsymbol{w}_n$ and the normal unit vector on the surface. The tensors, $w_{n,ij}$ and $\sigma_{n,ij}$, are the strain and stress tensors of the n-th mode, respectively. In order to calculate these tensors, $w_{n,i}$ is substituted for u_i in Eqs. (17) and (18) with $\phi = 0$. Equation (20) is valid when the integral of the function, $\sum_{i,j} w_{n,i}\phi\sigma_{k,ij}n_j$, on the surface of the elastic body vanishes. For example, the surface is fixed ($w_{n,i} = 0$) or free ($\sum_j \sigma_{k,ij}n_j = 0$) [27].

The equation of motion in the advanced modal expansion coincides with that in the traditional modal expansion when all of the couplings vanish. A comparison between Eqs. (9) and (16) shows that in viscous damping all α_{nk} ($n \neq k$) are zero when the dissipation strength, $\Gamma(\boldsymbol{r})$, does not depend on the position, $\boldsymbol{r}$. In the case of structure damping, from Eqs. (5)–(7) and (19), the stress, σ'_{ij}, without dissipation satisfies

$$\sum_j \frac{\partial\tilde{\sigma}'_{ij}}{\partial x_j} = -\sum_n \rho\omega_n{}^2 w_{n,i}\tilde{q}_n. \tag{21}$$

According to Eq. (9), Eq. (21) is decomposed without any couplings. From Eq. (21) and the structure damping term, $-i\sum_j \partial\phi(\boldsymbol{r})\tilde{\sigma}'_{ij}/\partial x_j$, the conclusion is derived; all of the couplings in the structure damping vanish when the loss amplitude, ϕ, is homogeneous. In summary, the inhomogeneous viscous and structure dampings produce mode couplings and destroy the traditional modal expansion.

The reason why the inhomogeneity of the loss causes the couplings is as follows. Let us consider the decay motion after only one resonant mode is excited. If the loss is uniform, the shape of the displacement of the system does not change while the resonant motion decays. On the other hand, if the dissipation is inhomogeneous, the

motion near the concentrated loss decays more rapidly than the other parts. The shape of the displacement becomes different from that of the original resonant mode. This implies that the other modes are excited, i.e. the energy of the original mode is leaked to the other modes. This energy leakage represents the couplings in the equation of motion.

It must be noticed that some kinds of "homogeneous" loss cause the couplings. For example, in thermoelastic damping [28–31], which is a kind of internal loss, the energy components of the shear strains $w_{n,ij}$ $(i \neq j)$ are not dissipated. The couplings α_{nk} do not have any terms that consist of the shear strain tensors. The coupling formula of the homogeneous thermoelastic damping is different from Eq. (20) with the constant ϕ. The couplings are not generally zero, even if the thermoelastic damping is uniform. The advanced, not traditional, modal expansion provides a correct evaluation of the homogeneous thermoelastic damping. In this paper, however, only coupling caused by inhomogeneous loss is discussed.

D. Thermal-noise formula of advanced modal expansion

In the advanced modal expansion, the transfer function, H_X, is derived from Eqs. (2), (10), and (14) (since the dissipation is small, only the first-order of α_{nk} is considered [32]),

$$H_X(\omega) = \sum_n \frac{1}{-m_n\omega^2 + m_n{\omega_n}^2(1 + i\phi_n)} - \sum_{k\neq n} \frac{i\alpha_{nk}}{[-m_n\omega^2 + m_n{\omega_n}^2(1 + i\phi_n)][-m_k\omega^2 + m_k{\omega_k}^2(1 + i\phi_k)]}. \quad (22)$$

Putting Eq. (22) into Eq. (1), the formula for the thermal noise is obtained. In the off-resonance region, where $|-\omega^2 + {\omega_n}^2| \gg {\omega_n}^2\phi_n(\omega)$ for all n, this formula approximates the expression

$$G_X(f) = \sum_n \frac{4k_BT}{m_n\omega} \frac{{\omega_n}^2\phi_n(\omega)}{(\omega^2 - {\omega_n}^2)^2} + \sum_{k\neq n} \frac{4k_BT}{m_nm_k\omega} \frac{\alpha_{nk}}{(\omega^2 - {\omega_n}^2)(\omega^2 - {\omega_k}^2)}. \quad (23)$$

The first term is the same as the formula of the traditional modal expansion, Eq. (13).

The interpretation of Eq. (23) is as follows. The power spectrum density of the thermal-fluctuation force of the n-th mode, G_{F_n}, and the cross-spectrum density between F_n and F_k, $G_{F_nF_k}$, are evaluated from Eq. (14) and the fluctuation-dissipation theorem [20,21]

$$G_{F_n}(f) = 4k_BT\frac{m_n{\omega_n}^2\phi_n(\omega)}{\omega}, \quad (24)$$

$$G_{F_nF_k}(f) = 4k_BT\frac{\alpha_{nk}(\omega)}{\omega}. \quad (25)$$

The power spectrum density G_{F_n} is independent of α_{nk}. On the other hand, $G_{F_nF_k}$ depends on α_{nk}. Having the correlations between the fluctuation forces of the modes, correlations between the motion of the modes must also exist. The power spectrum density of the fluctuation of q_n, G_{q_n}, and the cross-spectrum density between the fluctuations of q_n and q_k, $G_{q_nq_k}$, are described as [20,21]

$$G_{q_n}(f) = \frac{4k_BT}{m_n\omega} \frac{{\omega_n}^2\phi_n(\omega)}{(\omega^2 - {\omega_n}^2)^2}, \quad (26)$$

$$G_{q_nq_k}(f) = \frac{4k_BT}{m_nm_k\omega} \frac{\alpha_{nk}}{(\omega^2 - {\omega_n}^2)(\omega^2 - {\omega_k}^2)}, \quad (27)$$

under the same approximation of Eq. (23). The first and second terms in Eq. (23) are summations of the fluctuation motion of each mode, Eq. (26), and the correlations, Eq. (27), respectively. In conclusion, inhomogeneous mechanical dissipation causes mode couplings and correlations of the thermal motion between the modes.

In order to check whether the formula of the thermal motion in the advanced modal expansion is consistent with the equipartition principle, the mean square of the thermal fluctuation $\overline{X^2}$, which is an integral of the power spectrum density over the whole frequency region, is evaluated. This mean square is derived from Eq. (1) using the Kramers-Kronig relation [21,33]

$$\mathrm{Re}\,[H_X(\omega)] = -\frac{1}{\pi}\int_{-\infty}^{\infty} \frac{\mathrm{Im}[H_X(\xi)]}{\xi - \omega} d\xi. \quad (28)$$

The calculation used to evaluate the mean square is written as [21]

$$\overline{X^2} = \int_0^\infty G_X(f)df = \frac{1}{4\pi}\int_{-\infty}^{\infty} G_X(\omega)d\omega = -\frac{k_BT}{\pi}\int_{-\infty}^{\infty} \frac{\mathrm{Im}[H_X(\omega)]}{\omega} d\omega = k_BT\,\mathrm{Re}[H_X(0)]. \quad (29)$$

Since the transfer function, H_X, is the ratio of the Fourier components of the real functions, the value $H_X(0)$ is a real number. The functions ϕ_n and α_{nk}, which cause the imaginary part of H_X, must vanish when ω is zero [21]. The correlations do not affect the mean square of the thermal fluctuation. Equation (29) is rewritten using Eq. (22) as

$$\overline{X^2} = \sum_n \frac{k_B T}{m_n {\omega_n}^2}. \quad (30)$$

Equation (30) is equivalent to the prediction of the equipartition principle.

The calculation of the formula of the advanced modal expansion, Eq. (23), is more troublesome than that of the other methods [14–17], which are completely different from the modal expansion, when many modes contribute to the thermal motion. However, the advanced modal expansion gives clear physical insight about the discrepancy between the thermal motion and the traditional modal expansion, as shown in Sec. IV. It is difficult to find this insight using other methods.

III. EXPERIMENTAL CHECK

In order to test the advanced modal expansion experimentally, our previous experimental results concerning oscillators with inhomogeneous losses [8,12] are compared with an evaluation of the advanced modal expansion [17]. In an experiment involving a drum (a hollow cylinder made from aluminum alloy as the prototype of the mirror in the interferometer) with inhomogeneous eddy-current damping by magnets [12], the measured values agreed with the formula of the direct approach [14], Eq. (6) in Ref. [12]. This expression is the same as that of the advanced modal expansion [17].

Figure 2 presents the measured spectra of an aluminum alloy leaf spring with inhomogeneous eddy-current damping [8]. The position of the magnets for the eddy-current damping and the observation point are indicated above each graph. In the figures above each graph, the left side of the leaf spring is fixed. The right side is free. The open circles in the graphs represent the power spectra of the thermal motion derived from the measured transfer functions using the fluctuation-dissipation theorem. These values coincide with the directly measured thermal-motion spectra [8]. The solid lines are estimations using the advanced modal expansion (the correlations derived from Eqs. (16) and (27) are almost perfect [17]). As a reference, an evaluation of the traditional modal expansion is also given (dashed lines). The results of a leaf-spring experiment are consistent with the advanced modal expansion. Therefore, our two experiments support the advanced modal expansion.

IV. PHYSICAL INSIGHT GIVEN BY THE ADVANCED MODAL EXPANSION

The advanced modal expansion provides physical insight about the disagreement between the real thermal motion and the traditional modal expansion. Here, let us discuss the three factors that affect this discrepancy: the number of the modes, the absolute value and the sign of the correlation.

A. Number of modes

Since the difference between the advanced and traditional modal expansions is the correlations between the multiple modes, the number of the modes affects the magnitude of the discrepancy. If the thermal fluctuation is dominated by the contribution of only one mode, this difference is negligible, even when there are strong correlations. On the other hand, if the thermal motion consists of many modes, the difference is larger when the correlations are stronger.

Examples of the one-mode oscillator are given in Fig. 2. The measured thermal-motion spectra of the leaf spring with inhomogeneous losses below 100 Hz were the same as the estimated values of the ''traditional'' modal expansion. This is because these fluctuations were dominated by only the first mode (about 60 Hz). As another example, let us consider a single-stage suspension for a mirror in an interferometric gravitational-wave detector. The sensitivity of the interferometer is limited by the thermal noise of the suspensions between 10 Hz and 100 Hz. Since, in this frequency region, this thermal noise is dominated by only the pendulum mode [7], the thermal noise generated by the inhomogeneous loss agrees with the traditional modal expansion. It must be noticed that the above discussion is valid only when the other suspension modes are negligible. For example, when the laser beam spot on the mirror surface is shifted, the two modes (pendulum mode and mirror rotation mode) must be taken into account. In such cases, the inhomogeneous loss causes a disagreement between the real thermal noise of the single-stage suspension and the traditional modal expansion [34].

The discrepancy between the actual thermal motion and the traditional modal expansion in the elastic modes of the mirror [24] is larger than that of the drum, the prototype of the real mirror in our previous experiment [12]. One of the reasons is that the thermal motion of the mirror (rigid cylinder) consists of many modes [22,23]. The drum (hollow cylinder) had only two modes [12]. Since the number of modes that contribute to the thermal noise of the mirror in the interferometer increases when the laser beam radius becomes smaller [22,23], the discrepancy is larger with a narrower beam. This consideration is consistent with our previous calculation [24].

B. Absolute value of the correlation

In Eq. (27), the absolute value of the cross-spectrum density, $G_{q_n q_k}$, is proportional to that of the coupling, α_{nk}. Eqs. (16) and (20) show that the coupling depends on the scale of the dissipation distribution. A simple example of viscous damping is shown in Fig. 3. Let us consider the absolute value of α_{nk} when the viscous damping is concentrated (at around $\boldsymbol{r}_{\mathrm{vis}}$) in a smaller volume ($\Delta V$) than the wavelengths of the n-th and k-th modes. An example of this case is (A) in Fig. 3. It is assumed that the vector $\boldsymbol{w}_n(\boldsymbol{r}_{\mathrm{vis}})$ is nearly parallel to $\boldsymbol{w}_k(\boldsymbol{r}_{\mathrm{vis}})$. The absolute value of

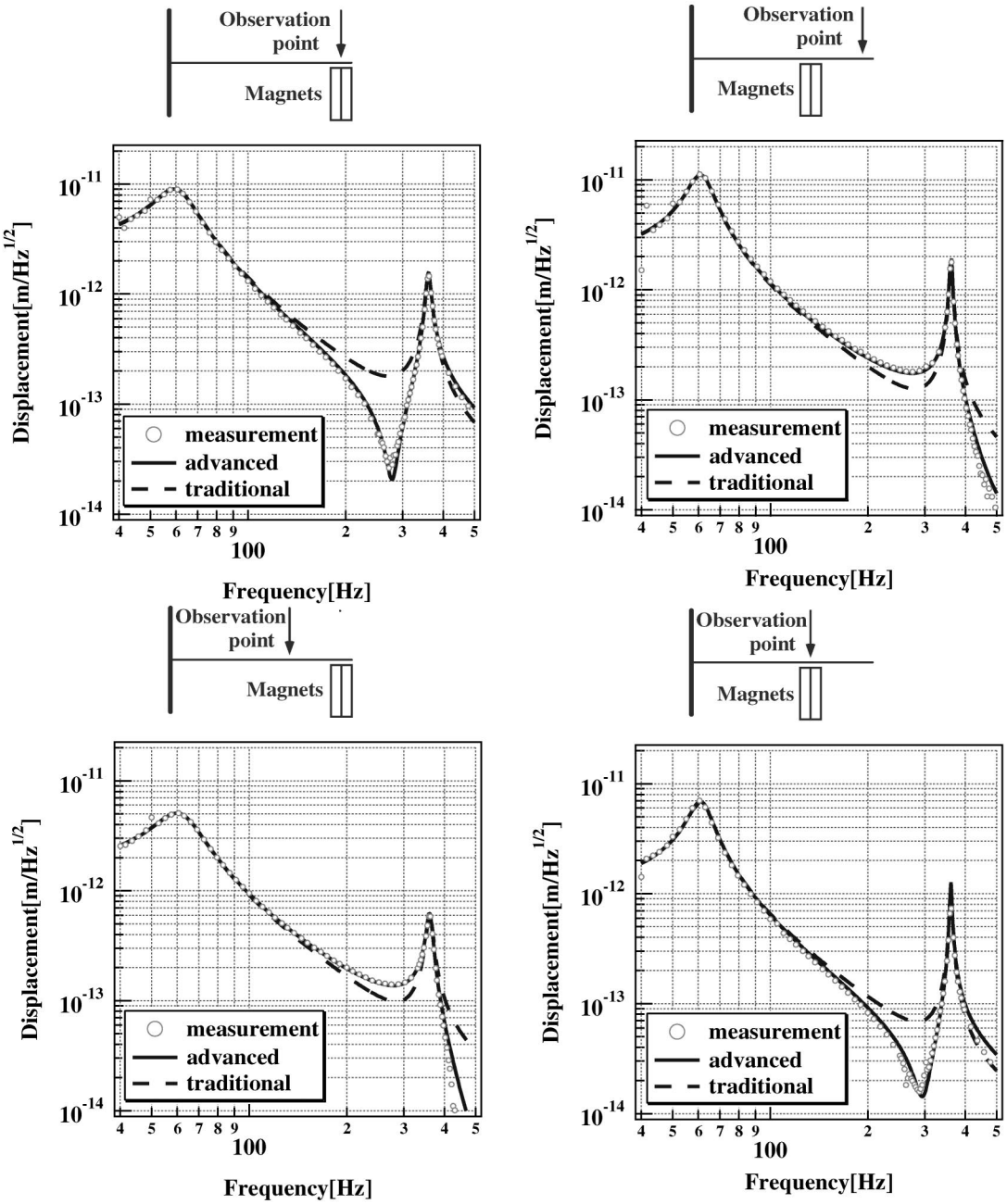

FIG. 2. Comparison between the estimated advanced modal expansion and the experimental results of an aluminum alloy leaf spring with inhomogeneous eddy-current damping [8]. The position of the magnets for the eddy-current damping and the observation point are indicated above each graph. In the figures above each graph, the left side of the leaf spring is fixed. The right side is free. The open circles in the graphs represent the power spectra of the thermal motion derived from the measured transfer functions using the fluctuation-dissipation theorem. These values coincide with the directly measured thermal-motion spectra [8]. The solid lines are estimations using the advanced modal expansion. As a reference, an evaluation of the traditional modal expansion is also given (dashed lines).

the coupling is derived from Eqs. (15) and (16) as

$$|\alpha_{nk}| \sim |\omega\rho\Gamma(\boldsymbol{r}_{\mathrm{vis}})\boldsymbol{w}_n(\boldsymbol{r}_{\mathrm{vis}})\cdot\boldsymbol{w}_k(\boldsymbol{r}_{\mathrm{vis}})\Delta V| \sim \sqrt{\omega\rho\Gamma(\boldsymbol{r}_{\mathrm{vis}})|\boldsymbol{w}_n(\boldsymbol{r}_{\mathrm{vis}})|^2\Delta V}\sqrt{\omega\rho\Gamma(\boldsymbol{r}_{\mathrm{vis}})|\boldsymbol{w}_k(\boldsymbol{r}_{\mathrm{vis}})|^2\Delta V}$$
$$\sim \sqrt{\alpha_{nn}\alpha_{kk}} = \sqrt{m_n\omega_n{}^2\phi_n m_k\omega_k{}^2\phi_k}. \tag{31}$$

The absolute value of the cross-spectrum is derived from Eqs. (26), (27), and (31) as

$$|G_{q_n q_k}| \sim \sqrt{G_{q_n} G_{q_k}}. \tag{32}$$

In short, the correlation is almost perfect [35]. On the other hand, if the loss is distributed more broadly than the wavelengths, the coupling—i.e. the correlation—is about zero

$$|G_{q_n q_k}| \sim 0. \tag{33}$$

The dissipation in the case where the size is larger than the wavelengths is equivalent to the homogeneous loss. An example of this case is (B) in Fig. 3. Although the above discussion is for the case of viscous damping, the conclusion is also valid for other kinds of dissipation. When the loss is localized in a small region, the correlations among many modes are strong. The loss in a narrower volume causes a larger discrepancy between the actual thermal motion and the traditional modal expansion. This conclusion coincides with our previous calculation of a mirror with inhomogeneous loss [24].

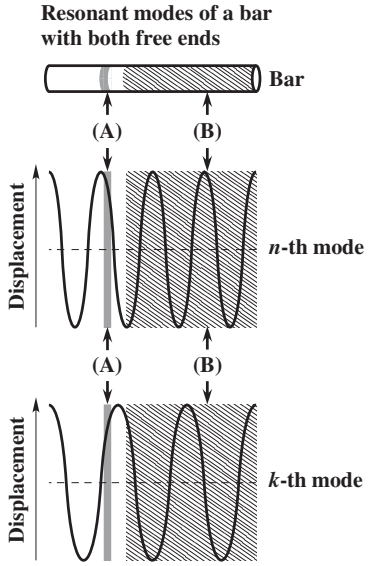

FIG. 3. Example for considering the absolute value of the coupling. There are the n-th and k-th modes $\boldsymbol{w}_n$ and $\boldsymbol{w}_k$ of a bar with both free ends. The vertical axis is the displacement. The dashed horizontal lines show the bar that does not vibrate. When only the gray part (A), which is narrower than the wavelengths on the left-hand side, has viscous damping, the absolute value of the coupling, Eq. (16), is large. Because the signs of $\boldsymbol{w}_n$ and $\boldsymbol{w}_k$ do not change in this region. If viscous damping exits only in the hatching part (B), which is wider than the wavelengths on the right-hand side, the coupling is about zero, because, in this wide region, the sign of the integrated function in Eq. (16), which is proportional to the product of $\boldsymbol{w}_n$ and $\boldsymbol{w}_k$, changes.

C. Sign of correlation

The sign of the correlation depends on the frequency, the loss distribution, and the position of the observation area. The position dependence provides a solution to the inverse problem: an evaluation of the distribution and frequency dependence of the loss from measurements of the thermal motion.

1. Frequency dependence

According to Eq. (27), the sign of the correlation reverses at the resonant frequencies. For example, in calculating the double pendulum [18], experiments involving the drum [12] and a resonant gravitational-wave detector with optomechanical readout [10], this change of the sign was found. In some cases, the thermal-fluctuation spectrum changes drastically around the resonant frequencies. A careful evaluation is necessary when the observation band includes the resonant frequencies. Examples are when using wide-band resonant gravitational-wave detectors [36–39], and thermal-noise interferometers [11,13]. The reason for the reverse at the resonance is that the sign of the transfer function of the mode with a small loss from the force (F_n) to the motion (q_n), H_n in Eq. (12) [$\propto (-\omega^2 + {\omega_n}^2)^{-1}$], below the resonance is opposite to that above it.

Since the sign of the correlation changes at the resonant frequencies, the cross-spectrum densities, the second term of Eq. (23), make no contribution to the integral of the power spectrum density over the whole frequency region, i.e. the mean square of the thermal fluctuation $\bar{X}^2$, as shown in Sec. II D. Therefore, the consideration in Sec. II D indicates that a reverse of the sign of the correlation conserves the equipartition principle, a fundamental principle in statistical mechanics.

2. Loss and observation area position dependence

According to Eqs. (16) and (20), and the normalization condition, Eq. (8) [40], the sign of the coupling, α_{nk}, depends on the loss distribution and the position of the observation area. A simple example is shown in Fig. 4. Owing to this normalization condition, near the observation area, the basis functions, $\boldsymbol{w}_n$, are similar in most cases. On the contrary, in a volume far from the observation area, $\boldsymbol{w}_n$ is different from each other in many cases. From Eqs. (8), (16), (20), and (25), when the loss is concentrated near to the observation area, most of the couplings (and the correlations between the fluctuation forces of the modes, $G_{F_n F_k}$) are positive. On the other hand, when the loss is localized far from the observation area, the numbers of the negative couplings and $G_{F_n F_k}$ are about the same as the positive ones. In such a case, most of the couplings between the n-th and $(n \pm 1)$-th modes (and $G_{F_n F_{n\pm1}}$) are negative. These are because the localized loss tends to apply to the fluctuation force on all of the modes to the

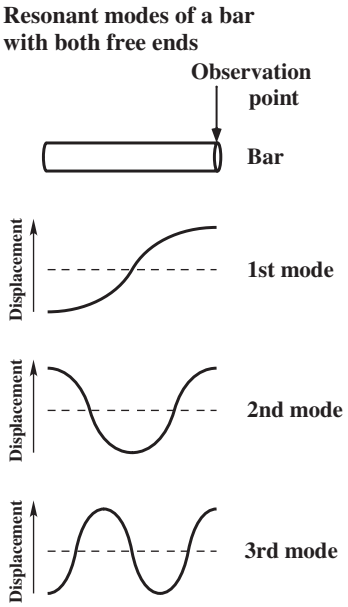

FIG. 4. Example for considering the sign of the coupling. There are the lowest three modes $\boldsymbol{w}_n$ of a bar with both free ends. The vertical axis is the displacement. The dashed horizontal lines show the bar that does not vibrate. The observation point is at the right-hand side end. The normalization condition is Eq. (8) [40]. The sign and shape of the displacement of all the modes around the observation point are positive and similar, respectively. On the contrary, at the left-hand side end, the sign and shape of the n-th mode are different from each other in many cases. From Eqs. (8), (16), and (20), when the loss is concentrated near to the observation area, most of the couplings are positive. On the other hand, when the loss is localized far from the observation area, the number of the negative couplings is about the same as the positive one. In such a case, most of the couplings between the n-th and $(n \pm 1)$-th modes are negative.

same direction around itself. Equation (27) indicates that the sign of the correlation, $G_{q_n q_k}$, is the same as that of the coupling, α_{nk}, below the first resonance. In this frequency band, the thermal motion is larger and smaller than the evaluation of the traditional modal expansion if the dissipation is near and far from the observation area, respectively. This conclusion is consistent with the qualitative discussion of Levin [14], our previous calculation of the mirror [24], and the drum experiment [12].

3. Inverse problem

The above consideration about the sign of the coupling gives a clue to solving the inverse problem: estimations of the distribution and frequency dependences of the loss from the measurement of the thermal motion. Since the sign of the coupling depends on the position of the observation area and the loss distribution, a measurement of the thermal vibrations at multiple points provides information about the couplings, i.e. the loss distribution. Moreover, multiple-point measurements reveal the loss frequency dependence. Even if the loss is uniform, the difference between the actual thermal motion and the traditional modal expansion exits when the expected frequency dependence of the loss angles, $\phi_n(\omega)$, is not correct [18]. The measurement at the multiple points shows whether the observed difference is due to an inhomogeneous loss or an invalid loss angle. This is because the sign of the difference is independent of the position of the observation area if the expected loss angles are not valid.

As an example, our leaf-spring experiment [8] is discussed. The two graphs on the right (or left) side of Fig. 2 show thermal fluctuations at different positions in the same mechanical system. The spectrum is smaller than the traditional modal expansion. The other one is larger. Thus, the disagreement in the leaf-spring experiment was due to inhomogeneous loss, not invalid loss angles. When the power spectrum had a dip between the first (60 Hz) and second (360 Hz) modes, the sign of the correlation $G_{q_1 q_2}$ was negative. According to Eq. (27), the sign of the coupling α_{12} was positive. The loss was concentrated near to the observation point when a spectrum dip was found. The above conclusion agrees with the actual loss shown in Fig. 2.

V. CONCLUSION

The traditional modal expansion has frequently been used to evaluate the thermal noise of mechanical systems [7]. However, recent experimental research [8–13] has proved that this method is invalid when the mechanical dissipation is distributed inhomogeneously. In this paper, we introduced a modification of the modal expansion [17,18]. According to this method (the advanced modal expansion), inhomogeneous loss causes correlations between the thermal fluctuations of the modes. The fault of the traditional modal expansion is that these correlations are not taken into account. Our previous experiments [8,12] concerning the thermal noise of the inhomogeneous loss support the advanced modal expansion.

The advanced modal expansion gives interesting physical insight about the difference between the actual thermal noise and the traditional modal expansion. When the thermal noise consists of the contributions of many modes, the loss is localized in a narrower area, which makes a larger difference. When the thermal noise is dominated by only one mode, this difference is small, even if the loss is extremely inhomogeneous. The sign of this difference depends on the frequency, the distribution of the loss, and the position of the observation area. It is possible to derive the distribution and frequency dependence of the loss from measurements of the thermal vibrations at multiple points.

There were many problems concerning the thermal noise caused by inhomogeneous loss. Our previous work [8,12,24] and this research solved almost all of these problems: a modification of the traditional estimation

method (in this paper), experimental checks of the new and traditional estimation methods and a confirmation of the new methods (Refs. [8,12] and this paper), an evaluation of the thermal noise of the gravitational-wave detector using the new method [24], and a consideration of the physical properties of the discrepancy between the actual thermal noise and the traditional estimation method (in this paper).

ACKNOWLEDGMENTS

This research was supported in part by the Japan Society for the Promotion of Science (for Young Scientists), and by a Grant-in-Aid for Creative Basic Research of the Ministry of Education.

[1] A. Abramovici *et al.*, Science **256**, 325 (1992).
[2] C. Bradaschia *et al.*, Nucl. Instrum. Methods Phys. Res., Sect. A **289**, 518 (1990).
[3] B. Willke *et al.*, Classical Quantum Gravity **19**, 1377 (2002).
[4] M. Ando *et al.*, Phys. Rev. Lett. **86**, 3950 (2001).
[5] K. Numata, A. Kemery, and J. Camp, Phys. Rev. Lett. **93**, 250602 (2004).
[6] M. Notcutt *et al.*, Phys. Rev. A **73**, 031804(R) (2006).
[7] P. R. Saulson, Phys. Rev. D **42**, 2437 (1990).
[8] K. Yamamoto, S. Otsuka, M. Ando, K. Kawabe, and K. Tsubono, Phys. Lett. A **280**, 289 (2001).
[9] G. M. Harry *et al.*, Classical Quantum Gravity **19**, 897 (2002).
[10] L. Conti, M. De Rosa, F. Marin, L. Taffarello, and M. Cerdonio, J. Appl. Phys. **93**, 3589 (2003).
[11] K. Numata, M. Ando, K. Yamamoto, S. Otsuka, and K. Tsubono, Phys. Rev. Lett. **91**, 260602 (2003).
[12] K. Yamamoto, S. Otsuka, Y. Nanjo, M. Ando, and K. Tsubono, Phys. Lett. A **321**, 79 (2004).
[13] E. D. Black *et al.*, Phys. Lett. A **328**, 1 (2004).
[14] Yu. Levin, Phys. Rev. D **57**, 659 (1998).
[15] N. Nakagawa, B. A. Auld, E. Gustafson, and M. M. Fejer, Rev. Sci. Instrum. **68**, 3553 (1997).
[16] K. Tsubono (unpublished).
[17] K. Yamamoto, Ph.D. thesis, The University of Tokyo, 2001 (http://t-munu.phys.s.u-tokyo.ac.jp/theses/yamamoto_d.pdf).
[18] E. Majorana and Y. Ogawa, Phys. Lett. A **233**, 162 (1997).
[19] H. B. Callen and R. F. Greene, Phys. Rev. **86**, 702 (1952).
[20] R. F. Greene and H. B. Callen, Phys. Rev. **88**, 1387 (1952).
[21] L. D. Landau and E. M. Lifshitz, *Statistical Physics* (Pergamon, New York, 1980), Part 1, Chap. 12, Sections 122, 123, 124, and 125.
[22] A. Gillespie and F. Raab, Phys. Rev. D **52**, 577 (1995).
[23] F. Bondu and J-Y. Vinet, Phys. Lett. A **198**, 74 (1995).
[24] K. Yamamoto, M. Ando, K. Kawabe, and K. Tsubono, Phys. Lett. A **305**, 18 (2002).
[25] Within the optics community, another revision of the modal expansion, the quasinormal modal expansion, is being discussed: A. M. van den Brink, K. Young, and M. H. Yung, J. Phys. A: Math Gen. **39**, 3725 (2006), and its references;
[26] J. J. Sakurai, *Modern Quantum Mechanics* (Benjamin/Cummings, California, 1985), Chap. 5.
[27] L. D. Landau and E. M. Lifshitz, *Theory of Elasticity* (Pergamon, New York, 1986), Chaps. 1, 3.
[28] C. Zener, Phys. Rev. **52**, 230 (1937); **53**, 90 (1938).
[29] V. B. Braginsky, M. L. Gorodetsky, and S. P. Vyatchanin, Phys. Lett. A **264**, 1 (1999).
[30] Y. T. Liu and K. S. Thorne, Phys. Rev. D **62**, 122002 (2000).
[31] M. Cerdonio, L. Conti, A. Heidmann, and M. Pinard, Phys. Rev. D **63**, 082003 (2001).
[32] In the off-resonance region, where $|-\omega^2+{\omega_n}^2| \gg {\omega_n}^2\phi_n(\omega)$ for all n, this approximation is always appropriate because the maximum of ${\alpha_{nk}}^2$ is $m_n{\omega_n}^2\phi_n m_k{\omega_k}^2\phi_k$ [35]. In the calculation to derive Eq. (22), Cramer's rule is useful.
[33] The sign on the right-hand side of the Kramers-Kronig relation in Ref. [21] is positive. The definition of the Fourier transformation in Ref. [21] is conjugate to that of this paper, Eq. (3).
[34] V. B. Braginsky, Yu. Levin, and S. P. Vyatchanin, Meas. Sci. Technol. **10**, 598 (1999).
[35] This discussion suggests that $|\alpha_{nk}|$ is never larger than $\sqrt{m_n{\omega_n}^2\phi_n m_k{\omega_k}^2\phi_k}$. The validity of this conjecture is supported by the Cauchy-Schwarz inequality [17].
[36] M. Cerdonio *et al.*, Phys. Rev. Lett. **87**, 031101 (2001).
[37] T. Briant *et al.*, Phys. Rev. D **67**, 102005 (2003).
[38] M. Bonaldi *et al.*, Phys. Rev. D **68**, 102004 (2003).
[39] M. Bonaldi *et al.*, Phys. Rev. D **74**, 022003 (2006).
[40] The results of the discussion presented in this section are valid under arbitrary normalization conditions. If a normalization condition other than Eq. (8) is adopted, the signs of some couplings change. The signs of the right-hand sides of Eqs. (10) and (14) also change. Eqs. (4)–(6) say that the right-hand sides of Eqs. (10) and (14) in the general style are $\sum_n q_n(t)\int \boldsymbol{w}_n(\boldsymbol{r})\cdot\boldsymbol{P}(\boldsymbol{r})dS$ and $\tilde{F}\int \boldsymbol{w}_n(\boldsymbol{r})\cdot\boldsymbol{P}(\boldsymbol{r})dS$, respectively. The change in the sign cancels each other in the process of the calculation for the transfer function, H_X, and the power spectrum of the thermal motion, G_X.